How to cite: *Angew. Chem. Int. Ed.* **2021**, *60*, 9507–9515
International Edition: doi.org/10.1002/anie.202100934
German Edition: doi.org/10.1002/ange.202100934

Supramolecular Chemistry

AIE-Active Chiral [3]Rotaxanes with Switchable Circularly Polarized Luminescence

Wei-Jian Li, Qingyi Gu, Xu-Qing Wang, Dan-Yang Zhang, Yu-Te Wang, Xiao He, Wei Wang,* and Hai-Bo Yang*

Abstract: *The construction of circularly polarized luminescence (CPL) switches with multiple switchable emission states and high dissymmetry factors (g_{lum}) has attracted increasing attention due to their broad applications in diverse fields such as the development of smart devices and sensors. Herein, a new family of AIE-active chiral [3]rotaxanes were designed and synthesized, from which a novel CPL switching system was successfully constructed. The switching process was realized through the controlled motions of the chiral pillar[5]arene macrocycles along the axle through the addition or removal of the acetate anions, which not only modulated the chirality information transfer but also tuned the aggregations of the integrated [3]rotaxanes, thus resulting in reversible transformations between two emission states with both high photoluminescence quantum yields (PLQYs) and high dissymmetry factors (g_{lum}) values.*

Introduction

Attributed to its broad potential applications in photonics, smart sensors, high-resolution three-dimensional (3D) displays, and information technologies etc., intense research interests on circularly polarized luminescence (CPL) have been witnessed during past few decades.[1] Aiming at the achievement of both high photoluminescence quantum yields (PLQYs) and high dissymmetry factors (g_{lum}) for practical applications, diverse CPL materials, ranging from lanthanide complexes at the early stage[2] to aggregation-induced emission luminogens (AIEgens) more recently,[3] have been successfully developed. In particular, for some CPL materials, through the modification of their chemical structures, conformations or assembly states by external stimuli such as light,[4] pH changes[5] or chemical inputs,[6] their CPL performances could be well-tuned, thus resulting in CPL switching.[7] Since CPL switching offers an promising opportunity for the in situ regulation of different CPL emissive states without the need for repetitive bottom-up synthesis, which is of considerable interest for the development of smart devices and sensors, it is attracting increasing attention and becoming a research hotspot.

To date, in addition to the introduction of some classical stimuli-responsive sites, such as cyanostilbene for light irradiation[4b] or imidazole for metal coordination,[6a] to trigger the switching process, some novel design strategies for CPL switching have been also witnessed. For instance, on the basis of the cycloaddition/cleavage of a cinnamic acid moiety, Liu, Zhang and co-workers successfully realized photo-triggered CPL inversion.[4c] In addition, by introducing the concept of molecular shuttle, Cuerva, Blanco and co-workers demonstrated the successful construction of a [2]rotaxane-based CPL switch triggered by base or acid.[5d] However, in most cases reported so far, only on/off switching with relatively low g_{lum} at the on states and moderate cycling ability was achieved. Considering the requirements for practical uses, the construction of novel CPL switching systems with multiple switchable emission states and higher g_{lum} is highly desirable and under demand.

To achieve this goal, herein a novel design strategy was developed. Based on our ongoing interest in mechanically interlocked molecules (MIMs),[8] chiral rotaxanes with the controllable dynamic features were hypothesized to be employed as the key platform for CPL switching. Moreover, inspired by the rapid development of AIEgen-based CPL systems usually with both high g_{lum} and PLQY values at the mesoscopic level,[9] we envisioned that the introduction of the AIEgen unit into the rotaxanes would keep the emission on in the aggregated states upon the CPL switching process. According to such design strategy, novel chiral [3]rotaxanes with an AIEgen unit as the center of the axle were designed and synthesized. On the basis of the controllable stimuli-induced motions of the chiral wheels that not only modulate the chirality information transfer but also influence the aggregation of the integrated [3]rotaxanes, CPL switching between two emission states with g_{lum} values of $\pm 2.14 \times 10^{-3}$ and $\pm 1.36 \times 10^{-2}$ was successfully realized, making this system an attractive and promising candidate for practical applications.

---

[*] W.-J. Li, Dr. X.-Q. Wang, D.-Y. Zhang, Y.-T. Wang, Prof. Dr. W. Wang, Prof. Dr. H.-B. Yang
Shanghai Key Laboratory of Green Chemistry and Chemical Processes & Chang-Kung Chuang Institute, School of Chemistry and Molecular Engineering, East China Normal University
3663 N. Zhongshan Road, Shanghai 200062 (P. R. China)
E-mail: wwang@chem.ecnu.edu.cn

Dr. Q. Gu, Prof. Dr. X. He
Shanghai Engineering Research Center of Molecular Therapeutics and New Drug Development, School of Chemistry and Molecular Engineering, East China Normal University
3663 N. Zhongshan Road, Shanghai 200062 (P. R. China)
E-mail: xiaohe@phy.ecnu.edu.cn

Supporting information and the ORCID identification number(s) for the author(s) of this article can be found under: https://doi.org/10.1002/anie.202100934.

Results and Discussion

Design, Synthesis, and Characterizations of [3]Rotaxane 1

In our initial design strategy, in the targeted chiral [3]rotaxane **1**, the typical AIEgen 9,10-distyrylanthracene (DSA) unit,[10] which is responsive to the high PLQY in the aggregated state, was chosen as the core, two pillar[5]arene macrocycles (DEP[5]A), which featured interesting conformation-dependent planar chirality,[11] were selected as the wheel components and the stereogenic units. In addition, two thiourea moieties were inserted into the alkyl chain component as the binding sites. In the initial state, due to the stronger hydrogen bonding interactions between the thiourea moieties and the ethoxy group of the DEP[5]A macrocycles, the DEP[5]A wheels were expected to be located at the thiourea and adjacent methylene moieties (**State I**). Since the thiourea moieties could serve as excellent hydrogen-bonding donors, the addition of the acetate anion as hydrogen-bonding acceptor with higher binding affinity to the thiourea moiety than that of DEP[5]A would drive the translational motion of pillar[5]arene macrocycles from the thiourea to the neutral alkyl chain (**State II**). Furthermore, through the removal of the acetate anions in the form of NaOAc precipitate by adding Na^+, the movement of the wheel components back to the thiourea moieties would be achieved, thus resulting in a switchable chiral [3]rotaxane.[12] More importantly, along with this proposed switchable process, two key factors that might influence the CPL performance of the chiral [3]rotaxane might be tuned, which would result in the desired CPL switch. On one hand, the distance between the chiral DEP[5]A wheels and the DSA core decreased upon the switching from **State I** to **State II**, which possibly led to enhanced chirality information transfer from the stereogenic units to the AIEgen.[13] On the other hand, accompanied by such relocation of the chiral DEP[5]A wheels close to the DSA unit, the AIE behaviors of not only the DSA core but also the integrated chiral [3]rotaxane might be tuned, which would further alter the CPL performance (Figure 1).

With above proposal in mind, the preparation of the racemic [3]rotaxane **1** was first undertaken.[14] On the basis of the host-guest chemistry of DEP[5]A and alkyl chain moiety, the threading-followed-by-stoppering strategy was employed through the reaction of DSA-cored precursor **3** and 3, 5-bis(trifluoromethyl)phenyl isothiocyanate in the presence of DEP[5]A in a ratio of 1:10:10, which gave rise to the successful synthesis of **1** in a good yield (81 %) on a gram scale (Figure 2a). In addition, the corresponding axle compound **2** was prepared as a model compound in near quantitative yield (Scheme S2). The comparison of the ^1H NMR spectra of

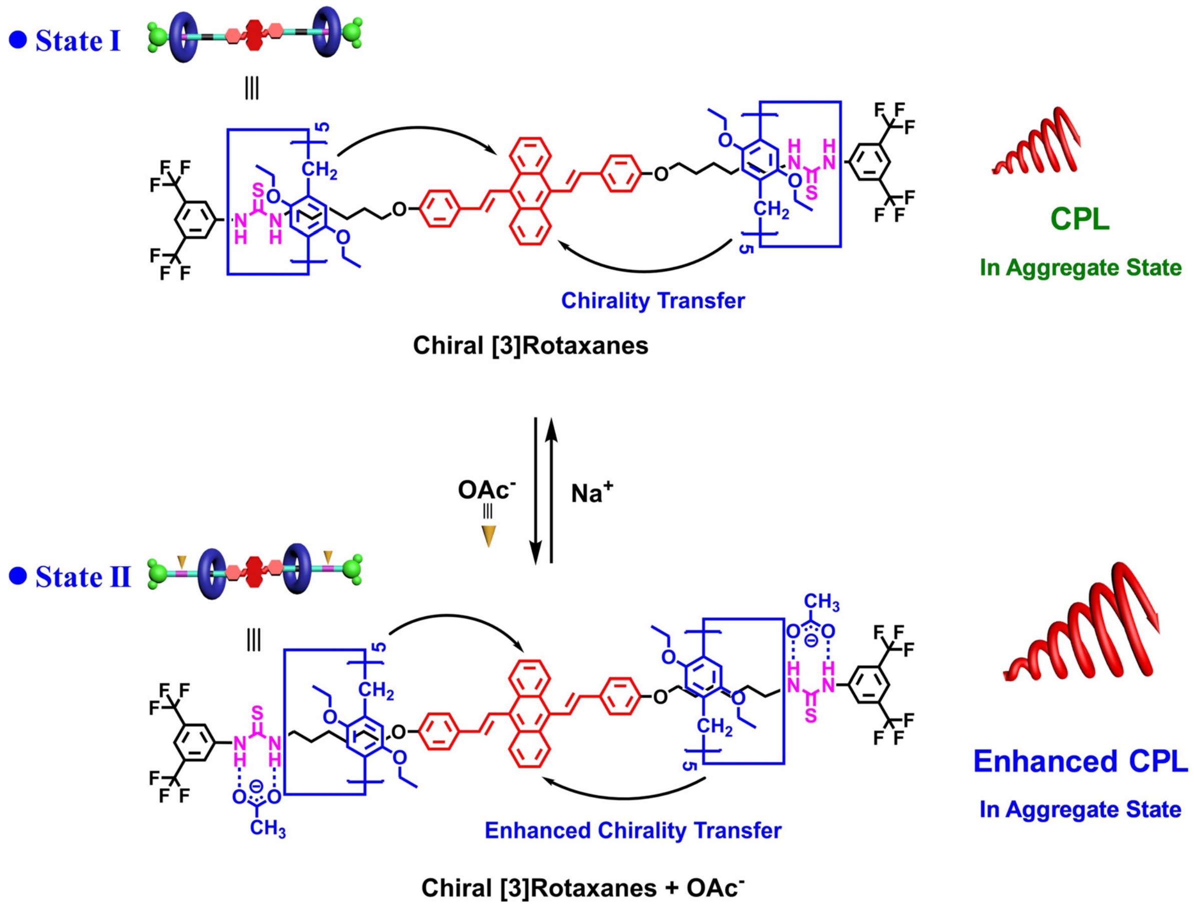

Figure 1. Design strategy of novel circularly polarized luminescence (CPL) switching system based on the AIE-active chiral [3]rotaxanes upon the addition or removal of external stimuli.

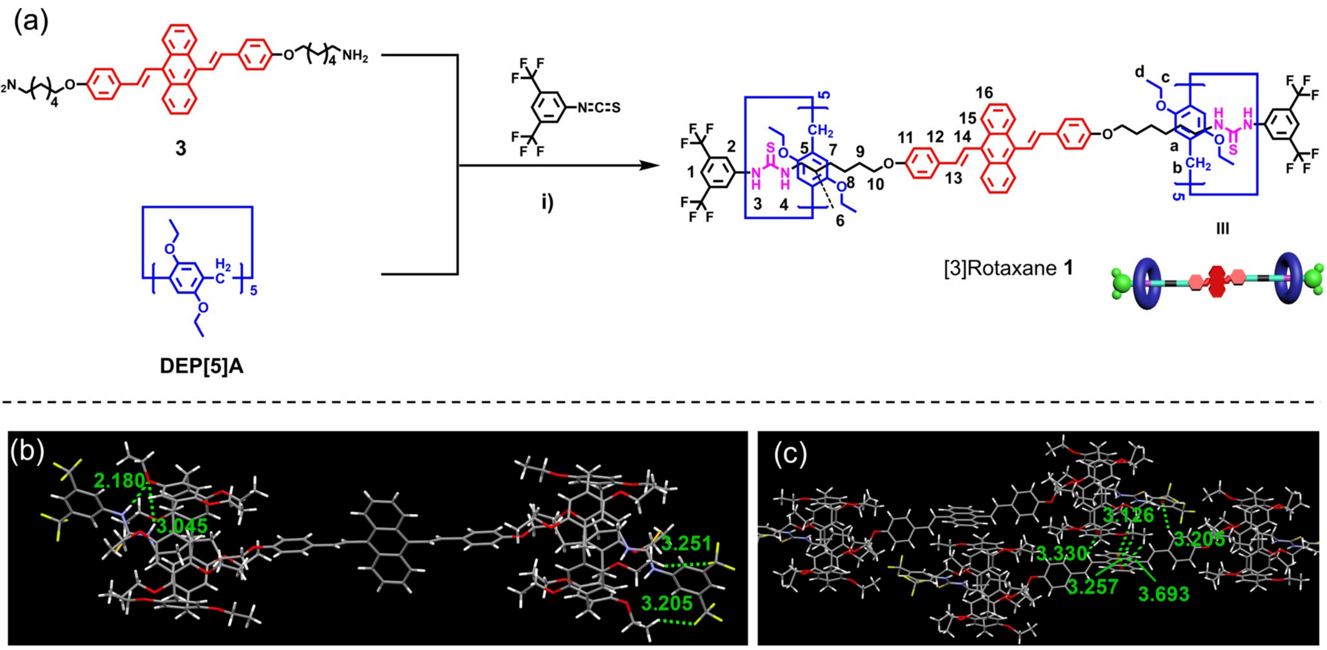

Figure 2. a) Synthetic route of [3]rotaxane **1**, and b,c) single crystal structure of [3]rotaxane **1** (the *meso*- form). i) $CHCl_3$, −15 °C to r.t., 81 %.

1 and **2** clearly indicated the formation of the targeted [3]rotaxane since remarkable upfield shifts of H_4 of the thiourea moiety and the methylene moiety ($H_{5\text{–}10}$) of the axle component were observed (Figure S13). In particular, three strongly upfield shifted signals below zero ppm were observed, which represents as typical indicators for the successful formation of the pillararene/alkyl chain rotaxane system. On the basis of two-dimensional (2D) COSY analysis (Figure S14), all signals of the axle were clearly assigned. In addition, as revealed by the 2D ROESY spectrum (Figure S15), correlations between protons on the axle and protons of DEP[5]A, for instance, $H_{6\text{–}9}$ with H_a, were observed, providing additional strong support for the formation of targeted [3]rotaxane. HRMS (ESI-TOF-MS) study further confirmed the existence of [3]rotaxane **1,** in which two peaks at $m/z = 2937.5288$ and $m/z = 1468.6790$ were observed, which were attributed to $[M]^+$ and $[M+2H]^{2+}$ ions, respectively (Figures S18,19).

By virtue of single-crystal X-ray diffraction, the structure of [3]rotaxane **1** was unambiguously confirmed. Single crystals suitable for crystallographic analysis were obtained by slow diffusion of acetone into the dichloromethane solution of **1**.[15] To our surprise, as revealed by the resultant single crystal structure, two pillar[5]arene wheels, one with (*pS*, *pS*, *pS*, *pS*, *pS*) conformation and the other with (*pR*, *pR*, *pR*, *pR*, *pR*) conformation, individually encircled the axle, affording [3]rotaxane **1** in the *meso* form (Detailed discussion of the absolute configurations of **1** will be given below). As expected, attributed to the hydrogen-bonding interactions between the thiourea moiety as well as the trifluoromethyl moiety and the ethoxy group of DEP[5]A, respectively, the DEP[5]A wheels were located at the thiourea and adjacent methylene moieties, which laid the foundation for the investigations of its stimuli-responsive feature discussed in the next section (Figure 2b). In addition, the DSA moiety was located in the center of the [3]rotaxane. In particular, due to the non-planarity of the DSA moiety and the presence of bulky DEP[5]A wheels that inhibited the typical cofacial π-π stacking, the CH/π interactions played a key role as the driving force in the crystal packing of *meso*-**1**. For instance, two intermolecular CH/π interactions formed between the anthrylene (An) core and the ethoxy group of DEP[5]A in neighboring rotaxane with the distances of 3.126, 3.257 and 3.693 Å, respectively. In addition, another two CH/π interactions are formed between the phenyl ring of DSA and the trifluoromethyl moiety (3.205 Å) as well as between the ethylene moiety of the DSA and the phenyl ring of the DEP[5]A (3.330 Å), respectively (Figure 2c). According to such packing form, the intermolecular interactions between the DSA unit and the DEP[5]A wheels were proven to have a great impact on the aggregation of the [3]rotaxane, making the modulation of the aggregation state as well as the CPL performance through stimuli-induced relocation of the DEP[5]A wheels feasible.

Stimuli-Responsive AIE Behaviors of [3]Rotaxane 1

With the targeted [3]rotaxane **1** in hand, investigations on its stimuli-responsive AIE behaviors were then carried out. To our delight, as suggested by the ^1H NMR titration experiments (Figure 3), the expected anion-induced translational motions of DEP[5]A macrocycles in [3]rotaxane **1** worked very well. Remarkable changes in the ^1H NMR spectra were observed upon the sequential addition of tetrabutylammonium acetate (TBAA) into the CD_2Cl_2 solution of **1**. In particular, significant downfield shifts of the signals of both the protons on the thiourea moieties (H_3 and H_4) and the adjacent methylene moieties ($H_{5\text{–}7}$) were revealed. Meanwhile, the signals of the methylene protons

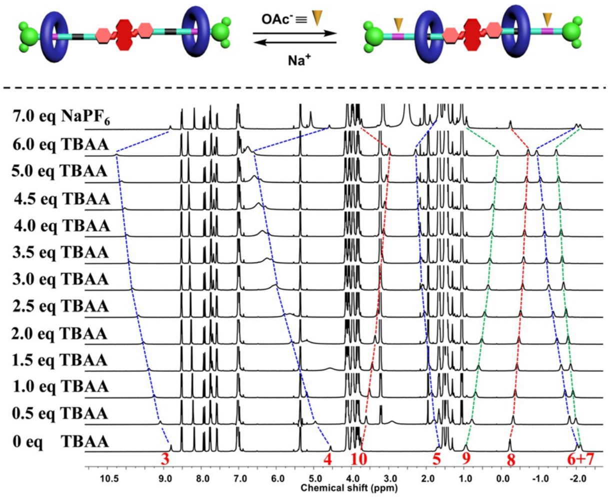

Figure 3. Cartoon representation (top) and ^{1}H NMR spectra (CD_2Cl_2, 298 K, 500 MHz) (bottom) of the anion-induced motions of the DEP[5]A macrocycles in [3]rotaxane **1**.

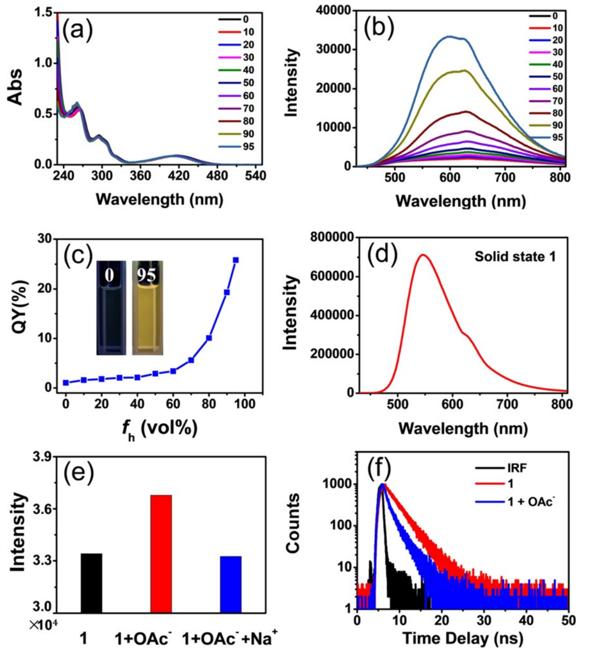

Figure 4. Stimuli-responsive AIE behaviors of [3]rotaxane **1**. a) UV-vis absorption, b) fluorescence spectra ($\lambda_{ex} = 415$ nm), c) fluorescence quantum yields, d) solid-state fluorescence spectra ($\lambda_{ex} = 415$ nm), e) stimuli-responsive fluorescence intensities and f) time-resolved fluorescence decay curves of [3]rotaxane **1**. Inset: photographs of **1** in CH_2Cl_2/n-hexane with 0% (left) and 95% (right) n-hexane fractions taken under UV illumination ($\lambda_{ex} = 365$ nm) (3 μM).

(H_{8-10}) close to the DSA moiety and the alkene protons (H_{13}) attributed to the DSA moiety were upfield shifted (Figures S27). For instance, after the addition of 6.0 equiv of TBAA, downfield shifts of the signals of protons H_3 and H_4 from 4.55 to 6.60 ppm and from 8.80 to 10.25 ppm, respectively, were observed. While the upfield shift of the signal of proton H_9 from 0.94 to 0.09 ppm was also revealed, clearly suggesting the translational motions of DEP[5]A macrocycles from the thiourea to the neutral alkyl chain. As expected, after the complete removal of the acetate anions as NaOAc precipitates through the subsequent addition of at least 7.0 equiv of $NaPF_6$ to the mixture of [3]rotaxane **1** and TBAA, the DEP[5]A macrocycles were returned to the thiourea moieties, as indicated by the nearly identical ^{1}H NMR spectrum as the original one. Notably, such reversible anion-induced switching motions of DEP[5]A wheels along the axle could be repeated at least five times without any degradation, demonstrating the excellent cycling ability (Figure S28). Moreover, to quantitatively evaluate this anion-induced switching process, the binding affinity of [3]rotaxane towards acetate anions was then evaluated. A 1:2 binding model (**1**: acetate anion) with anion binding constants of $K_1 = 142.1 \pm 5.6\ M^{-1}$ and $K_2 = 13.9 \pm 2.0\ M^{-1}$ were calculated, which was in accord with the existence of two thiourea moieties of [3]rotaxane **1** as binding sites (Figures S30–33). Notably, compared with that of some previously reported bis-thiourea receptors,[16] such binding constants are smaller, which might be caused by the competitive complexing of the DEP[5]A macrocycles with the thiourea moieties.

After confirming the anion-induced switching of the [3]rotaxane **1**, the evaluation of its stimuli-responsive AIE behavior was then performed. As shown in Figure 4, the absorption spectra of **1** in dilute CH_2Cl_2 solution (3 μM) were first recorded. Two main absorption bands at around 295 nm and 415 nm were observed, which corresponded to the pillar[5]arene moieties and the DSA core, respectively. Upon the increase of the fraction of poor solvent hexane (f_h, vol%) from 10% to 95%, only very slight hypochromic shifts were observed, indicating the absence of π-π interactions in the resultant aggregated state. Moreover, as revealed by the fluorescence spectra, in pure CH_2Cl_2 solution, [3]rotaxane **1** displayed very weak fluorescence with a fluorescence quantum yield (Φ_F) of 1.0 ± 0.1%. Upon gradually increasing f_h from 10% to 60%, the emission intensity only revealed a slight increase. By further increasing the f_h to 70% and finally to 95%, significant fluorescence emission enhancement was observed, as observed in the photographs of the solution of **1** with different f_h values taken under $\lambda = 365$ nm UV illumination (Figure 4c). As reflected by the Φ_F values, an impressive 26-fold enhancement (25.8 ± 1.2%) of the fluorescence quantum yield was observed when f_h was 95%, indicating that [3]rotaxane **1** is a typical AIE luminogen. Similar to [3]rotaxane **1**, the corresponding axle compound **2** also displayed typical AIE behaviors. However, compared with that of **1**, lower fluorescence emission enhancement (15-fold) was revealed, highlighting a unique effect of the formation of the [3]rotaxane (Figure S35). In addition, according to the fluorescence spectra in the solid state, both **1** and **2** revealed highly emissive feature in solid state with the fluorescence quantum yields of 36.6 ± 0.2% and 23.1 ± 1.3%, respectively. Such impressive emission features of **1** and **2** could be attributed to the existence of ordered packing to block intramolecular motions in the solid state, as confirmed by their sharp powder X-ray diffraction (PXRD) patterns (Figures S23,24).

More importantly, by keeping f_h at 95%, the addition of TBAA to induce DEP[5]A movement led to a further increase in the fluorescence emission intensity but a slight decrease of the Φ_F value to 24.3 ± 2.6 %. The sequential addition of Na^+ to remove the acetate anions resulted in the recovery of the emission intensity (Figure 4 e and Figure S39), indicating that such a reversible switching process did influence the AIE behaviors of [3]rotaxane **1**. Interestingly, for both **1** and **2**, as revealed by the fluorescence lifetimes that were recorded by the time-correlated single-photon counting (TCSPC) technique (Figure 4 f), a decrease of the fluorescence lifetimes upon the addition of TBAA (for **1**, from 3.20 ns to 1.50 ns; for **2**, from 3.22 ns to 2.74 ns, Figure S40 and Table S1) was observed, suggesting anion-induced co-conformational changes that influenced the energy of the excited states. It is also worth noting that the fluorescence lifetimes agree well with the mono-exponential decay model, indicating that the fluorescence originates from the sole excited state and no competing radiative deactivation process occurs.[17]

In order to provide more information for aforementioned stimuli-responsive AIE behaviors of **1**, dynamic light scattering (DLS) was further employed to investigate the different aggregation states of **1**. According to the DLS results, no aggregation of **1** was observed in pure CH_2Cl_2 solution with an average hydrodynamic diameter (D_h) of 1.5 ± 0.1 nm. When f_h was increased to 95 %, the average D_h remarkably increased to 65.5 ± 6.3 nm, clearly suggesting the formation of nanoscale aggregates. The sequential addition of TBAA to trigger the switching of **1** led to a further increase of the average D_h to 122.0 ± 8.6 nm, again confirming the anion-induced tuning of the AIE behavior of **1**. As expected, sequentially adding Na^+ to drive the reversed switching process resulted in the almost complete regeneration of the original aggregation state with an average D_h of 72.5 ± 4.7 nm (Figures S41).

Resolution of [3]Rotaxane 1

In principle, due to the existence of eight conformers (i.e., four diastereomers × two enantiomers) of DEP[5]A, there should be 36 isomers of [3]rotaxane **1** (Figure S45). However, as revealed by the chiral HPLC measurements, three peaks with a ratio of peak areas of 24.2:51.1:24.6 were observed, preliminarily indicating the existence of only three isomers in [3]rotaxane **1** (Figure 5 a,b). After isolation of these fractions using chiral preparative HPLC column, ^1H NMR analysis of each fraction was first performed. As shown in Figure S50, the ^1H NMR spectrum of the first fraction is almost the same as that of the third fraction, both of which are only slightly different from that of the second fraction, suggesting the isolation of the [3]rotaxane enantiomers. The CD analysis further confirmed such hypothesis, as the CD peak patterns of the first fraction and the third fraction mirrored each other in both form and intensity, which is consistent with an enantiomeric relationship. In addition, the second fraction revealed no CD signal, indicating that it is the *meso* form of [3]rotaxane **1** (Figure 5 c). The ratio of these three isomers was approximately about 1:2:1, which matches the statistical distributions. According to these results, the formation of [3]rotaxane **1** was proven to be diastereospecifical to symmetric diastereoisomers, possibly attributed to both the lower energy and larger cavity of DEP[5]A in the (*pS*, *pS*, *pS*, *pS*, *pS*) and (*pR*, *pR*, *pR*, *pR*, *pR*) conformers.[14e]

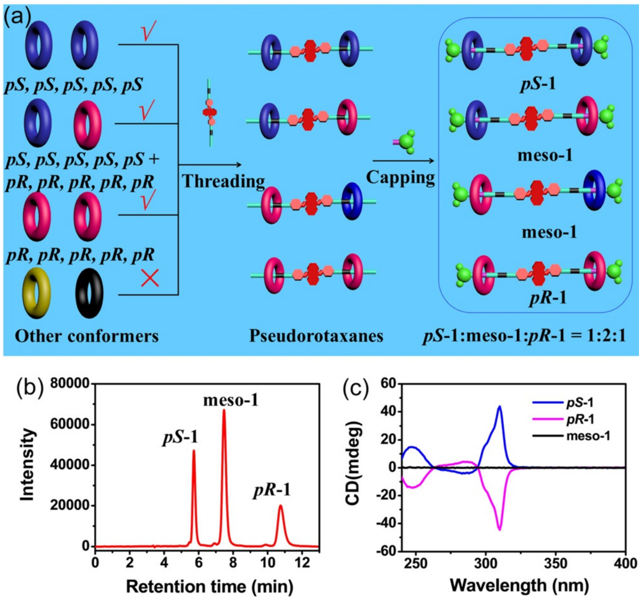

Figure 5. a) Cartoon representation of the diastereospecific formation of [3]rotaxane **1**, b) chiral HPLC traces, and c) CD spectra (50 μM in CH_2Cl_2) of the three fractions that were assigned to *pS*-**1**, *meso*-**1**, and *pR*-**1**, respectively.

More importantly, according to both the CD spectra and previous reports,[11b,14e] the absolute configurations of the [3]rotaxane in the first fraction (*pS*-**1**) and the third fraction (*pR*-**1**) were assigned to be *pS* and *pR*, respectively, in which both wheels threaded on the axle are in (*pS*, *pS*, *pS*, *pS*, *pS*) or (*pR*, *pR*, *pR*, *pR*, *pR*) conformers, respectively. While for the [3]rotaxane in the second fraction (*meso*-**1**), as revealed by its X-ray single crystal structure described above, one (*pS*, *pS*, *pS*, *pS*, *pS*) wheel and one (*pR*, *pR*, *pR*, *pR*, *pR*) wheel were located on the axle. Notably, due to the existence of the axle in the cavity of DEP[5]A that blocks the free rotations of the paraphenylene methylene units, all rotaxanes displayed high configuration stability. No racemization was observed even after prolonged heating (Figure S51), such stability makes them excellent candidates for novel CPL materials.

Switchable CPL of Chiral [3]Rotaxanes pS-1 *and* pR-1

With the targeted chiral [3]rotaxanes in hand, their chiroptical properties were then evaluated. The solution-state CD spectra of both *pS*-**1** and *pR*-**1** indicated that there was no obvious chirality information transfer even after the addition of acetate anions to trigger the DEP[5]A macrocycles to relocate near to the DSA unit, as revealed by the fact that only slight changes in the intensity of the bands at both 250 nm and 310 nm, which could be mainly attributed to the DEP[5]A macrocycles, were observed (Figure S52). Moreover, as suggested by the CD spectra of the cast film of *pS*-**1** and *pR*-**1** (Figure S53), bands at 250 nm and 310 nm were observed, which is consistent with the solution state CD spectra. However, a weak band at around 400 nm, which was ascribed to the DSA unit, was also observed, suggesting very weak chirality information transfer in **State I**. Moreover, upon the addition of acetate anions, the CD spectra of the resultant cast film of *pS*-**1** and *pR*-**1** in **State II** revealed an increase in the intensity of this band at around 400 nm, clearly indicating the expected stimuli-induced enhancement of chirality information transfer (Figure S54).

Encouraged by such stimuli-induced switching of the chirality information transfer from the planar chiral DEP[5]A macrocycles to the DSA unit as well as the intriguing emission features of the [3]rotaxanes, tests of the CPL of these two chiral [3]rotaxanes were then performed (Figure 6). To our delight, upon excitation with UV light ($\lambda_{ex} = 360$ nm), both *pS*-**1** and *pR*-**1** revealed intense CPL signals at 535 nm, which was attributed to the DSA units. As expected, these enantiomeric [3]rotaxanes resulted in almost mirror-imaged CPL signals with opposite g_{lum}, i.e., a positive CPL signal for the *pS*-**1** film was observed, while the film of *pR*-**1** revealed a negative signal, again suggesting a pure CPL response. The g_{lum} values for both chiral [3]rotaxanes were $\pm 2.14 \times 10^{-3}$, which is relatively large compared with the typical ranges ($\approx 10^{-5}$–10^{-3} order). More importantly, upon switching these chiral [3]rotaxanes to **State II** with enhanced chirality information transfer, an impressive increase in the g_{lum} value to $\pm 1.36 \times 10^{-2}$ was achieved, leading to a novel CPL switching system with a 6.4-fold enhancement. Moreover, this CPL switching system displayed excellent cycling ability. For both *pS*-**1** and *pR*-**1**, even after at least 5 cycles, no obvious degradation was observed (Figures S56,57).

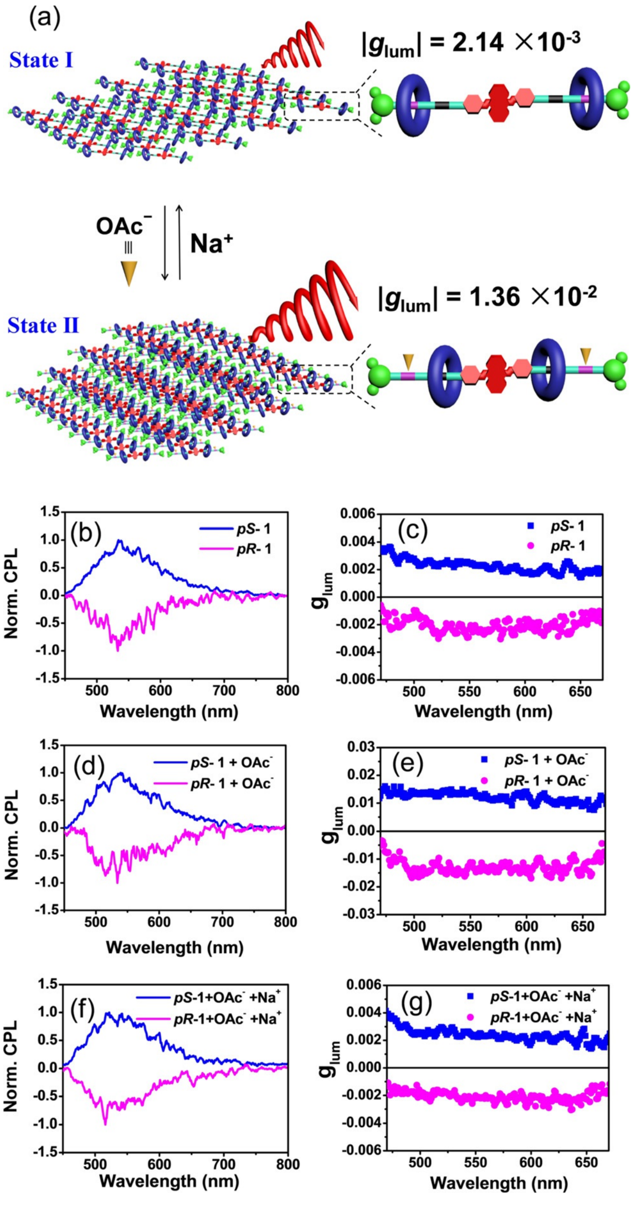

Figure 6. a) Cartoon representation of CPL switching system based on the anion-induced motions of the wheels in the chiral [3]rotaxanes, b,c) CPL spectra and g_{lum} spectra of the cast film of *pS*-**1** and *pR*-**1**, d,e) CPL spectra and g_{lum} spectra of the cast film of *pS*-**1** and *pR*-**1** upon the addition of TBAA, and f,g) CPL spectra and g_{lum} spectra of the cast film of *pS*-**1** and *pR*-**1** after the removal of TBAA using Na$^+$.

To gain a better understanding of such an attractive CPL switching system, extensive computational simulations[18] were then performed, and the details are shown in Section F in the Supporting Information. To our delight, as shown in Figure 7b, the simulated CPL spectra of *pS*-**1** fit very well with the experimental result, in which a positive CPL signal at 534 nm was revealed. More importantly, after the addition of acetate anions to trigger the switching process, a remarkable increase in the intensity of this CPL signal was suggested. Regarding the g_{lum}, the values can be roughly calculated as $4R/D$, where R and D are the rotational and dipole strengths, respectively, relative to the first electronic transition.[19] In our case, as listed in Table S5, upon the addition of acetate anions, a remarkable increase in the R value from 4.23 to 16.55 cgs and a slight decrease in the D value from 18.15 to 16.79 a.u. were calculated. According to these values, a 4.3-fold enhancement of the g_{lum} value after the acetate-induced switching process was predicted, which is close to the experimental result.

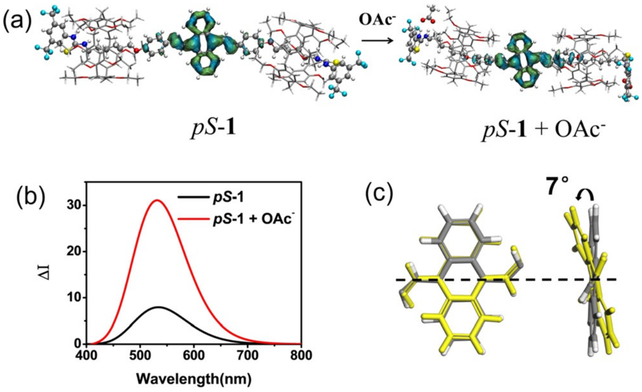

Figure 7. Mechanism of the CPL switching by TD-DFT calculations: a) Optimized excited-state structures of the chiral [3]rotaxane *pS*-**1** and and *pS*-**1** with the addition of two acetate anions for the distribution of the holes (cyan) and electrons (lime), b) simulated CPL spectra, and c) the change of dihedral of the 9,10-distyrylanthrance (DSA) unit of the chiral [3]rotaxane *pS*-**1** and *pS*-**1** with the addition of two acetate anions (the DSA unit in *pS*-**1** with the addition of two acetate anions was marked with yellow).

According to the simulations, the rotation of the dihedral of the DSA unit and the following electron-hole difference of the chiral [3]rotaxanes *pS*-**1** upon the addition of acetate anions was considered to lead to the enhancement of the g_{lum} value. As shown in Figure 7c, it was obvious that the DSA unit rotated and the dihedral of this AIEgen group enlarged with around 7°. The rotation of the DSA unit might occur because of the lower stability of the excited-state structure compared with the ground-state structure, thus the DSA unit was affected more by the motions of the chiral DEP[5]A macrocycles upon the addition of acetate anions. From the electron-hole analysis, the region of hole also appeared in the phenyl group of the DSA unit, which indicated the fluorescence enhancement of [3]rotaxane *pS*-**1** after the addition of acetate anions (Figure 7a).

The change in the dihedral of the DSA unit might further influence the aggregation behaviors of the chiral [3]rotaxanes, which could further contribute to the enhancement of the g_{lum} value. To evaluate such aggregation effect, atomic force microscopy (AFM) analysis was carried out. For chiral [3]rotaxane *pS*-**1** and *pR*-**1**, homogeneous tadpole-like morphology with slight cross-linking was observed, and the average heights were 5.6 ± 0.4 nm and 5.9 ± 0.5 nm for *pS*-**1** and *pR*-**1**, respectively. After the addition of acetate anions to induce the switching process, denser morphology with increased cross-linking was revealed, and the average heights increased to 14.3 ± 0.9 nm and 14.5 ± 0.9 nm for *pS*-**1** and *pR*-**1**, respectively (Figure 8). Such obvious acetate-induced morphology transformations to the denser state were hypothesized to enhance the intermolecular chirality information transfer, which might further contribute to the increase in the g_{lum} value.

Conclusion

In summary, taking advantage of the unique dynamic features of rotaxanes, a novel chiral [3]rotaxane-based CPL switching system was successfully constructed. The introduction of the DSA unit into the chiral [3]rotaxanes endowed them with high PLQY in both switching states. More impressively, on the basis of the anion-induced controllable motions of the chiral DEP[5]A wheels that not only enhanced the chirality information transfer but also tuned the aggregation behaviors of the integrated chiral [3]rotaxanes, an impressive switching between two CPL emission states of the chiral [3]rotaxanes with g_{lum} values of $\pm 2.14\times10^{-3}$ and $\pm 1.36\times10^{-2}$ was successfully realized. The relatively large g_{lum} values, the remarkable difference in the g_{lum} values, and the excellent cycling ability make the current CPL switching system an attractive candidate for the fabrication of smart devices and sensors. Considering the recent rapid development of chiral MIMs, especially chiral rotaxanes, and their wide potential applications,[20] our proof-of-concept study herein provides a feasible and promising approach that could be employed for the construction of diverse CPL switching systems, such as ones that could be operated in the solid state, which would lay the foundation for the further explorations of the practical applications of CPL switches.

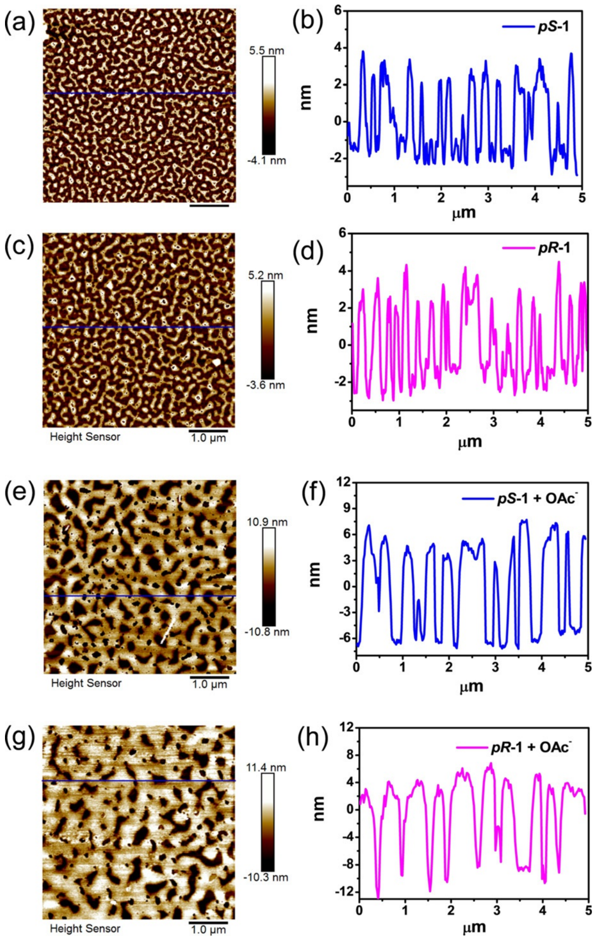

Figure 8. AFM images of the chiral [3]rotaxanes before and after the anion-induced switching process: a,b) *pS*-**1**, the average height is 5.6 ± 0.4 nm, c,d) *pR*-**1**, the average height is 5.9 ± 0.5 nm, e,f) *pS*-**1** with the addition of TBAA, the average height is 14.3 ± 0.9 nm, g,h) *pR*-**1** with the addition of TBAA, the average height is 14.5 ± 0.9 nm.

Acknowledgements

W.W. acknowledges the financial support sponsored by the National Natural Science Foundation of China (22001073), Shanghai Sailing Program (20YF1411500), and the Fundamental Research Funds for the Central Universities. H.-B.Y. acknowledges the financial support sponsored by the National Natural Science Foundation of China (21625202 and 92056203), the Innovation Program of Shanghai Municipal Education Commission (2019-01-07-00-05-E00012) and the Fundamental Research Funds for the Central Universities. X.H. acknowledges the financial support sponsored by the National Natural Science Foundation of China (Grant Nos. 21922301, 21761132022, and 21673074), the National Key R&D Program of China (Grant Nos. 2016YFA0501700, and 2019YFA0905201), Shanghai Municipal Natural Science Foundation (Grant No. 18ZR1412600), and the Fundamental Research Funds for the Central Universities. We also thank the Supercomputer Center of East China Normal University (ECNU Multifunctional Platform for Innovation 001) for providing computer resources.

Conflict of interest

The authors declare no conflict of interest.

Keywords: aggregation-induced emission · chiral rotaxanes · circularly polarized luminescence · pillar[5]arene · stimuli responsiveness

---

[1] a) G. Longhi, E. Castiglioni, J. Koshoubu, G. Mazzeo, S. Abbate, *Chirality* **2016**, *28*, 696; b) J. Han, S. Guo, H. Lu, S. Liu, Q. Zhao, W. Huang, *Adv. Opt. Mater.* **2018**, *6*, 1800538; c) E. M. Sánchez-Carnerero, A. R. Agarrabeitia, F. Moreno, B. L. Maroto, G. Muller, M. J. Ortiz, S. de la Moya, *Chem. Eur. J.* **2015**, *21*, 13488; d) Y. Sang, J. Han, T. Zhao, P. Duan, M. Liu, *Adv. Mater.* **2019**, *31*, 1900110; e) D.-W. Zhang, M. Li, C.-F. Chen, *Chem. Soc. Rev.* **2020**, *49*, 1331; f) T. Zhao, J. Han, P. Duan, M. Liu, *Acc. Chem. Res.* **2020**, *53*, 1279.

[2] a) *Luminescence of Lanthanide Ions in Coordination Compounds and Nanomaterials* (Ed.: A. de Bettencourt-Dias), Wiley, Hoboken, **2014**; b) F. Zinna, L. D. Bari, *Chirality* **2015**, *27*, 1; c) J. L. Lunkley, D. Shirotani, K. Yamanari, S. Kaizaki, G. Muller, *J. Am. Chem. Soc.* **2008**, *130*, 13814.

[3] a) J. Luo, Z. Xie, J. W. Y. Lam, L. Cheng, H. Chen, C. Qiu, H. S. Kwok, X. Zhan, Y. Liu, D. Zhu, B. Z. Tang, *Chem. Commun.* **2001**, 1740; b) B. Z. Tang, X. Zhan, G. Yu, P. P. S. Lee, Y. Liu, D. Zhu, *J. Mater. Chem.* **2001**, *11*, 2974; c) J. Mei, N. L. C. Leung, R. T. K. Kwok, J. W. Y. Lam, B. Z. Tang, *Chem. Rev.* **2015**, *115*, 11718; d) B. Liu, B. Z. Tang, *Angew. Chem. Int. Ed.* **2020**, *59*, 9788; *Angew. Chem.* **2020**, *132*, 9872; e) Z. Zhao, H. Zhang, J. W. Y. Lam, B. Z. Tang, *Angew. Chem. Int. Ed.* **2020**, *59*, 9888; *Angew. Chem.* **2020**, *132*, 9972; f) B. Jiang, C.-W. Zhang, X.-L. Shi, H.-B. Yang, *Chin. J. Polym. Sci.* **2019**, *37*, 372; g) L.-J. Chen, Y.-Y. Ren, N.-W. Wu, B. Sun, J.-Q. Ma, L. Zhang, H. Tan, M. Liu, X. Li, H.-B. Yang, *J. Am. Chem. Soc.* **2015**, *137*, 11725; h) J. Roose, B. Z. Tang, K. S. Wong, *Small* **2016**, *12*, 6495; i) Y. Shi, G. Yin, Z. Yan, P. Sang, M. Wang, R. Brzozowski, P. Eswara, L. Wojtas, Y. Zheng, X. Li, J. Cai, *J. Am. Chem. Soc.* **2019**, *141*, 12697; j) H. Qu, Y. Wang, Z. Li, X. Wang, H. Fang, Z. Tian, X. Cao, *J. Am. Chem. Soc.* **2017**, *139*, 18142; k) Q. Liao, Q. Gao, J. Wang, Y. Gong, Q. Peng, Y. Tian, Y. Fan, H. Guo, D. Ding, Q. Li, Z. Li, *Angew. Chem. Int. Ed.* **2020**, *59*, 9946; *Angew. Chem.* **2020**, *132*, 10032.

[4] a) Y. Hashimoto, T. Nakashima, D. Shimizu, T. Kawai, *Chem. Commun.* **2016**, *52*, 5171; b) X. Jin, D. Yang, Y. Jiang, P. Duan, M. Liu, *Chem. Commun.* **2018**, *54*, 4513; c) H. Jiang, Y. Jiang, J. Han, L. Zhang, M. Liu, *Angew. Chem. Int. Ed.* **2019**, *58*, 785; *Angew. Chem.* **2019**, *131*, 795.

[5] a) S. Tong, J.-T. Li, D.-D. Liang, Y.-E. Zhang, Q.-Y. Feng, X. Zhang, J. Zhu, M.-X. Wang, *J. Am. Chem. Soc.* **2020**, *142*, 14432; b) K. Takaishi, M. Yasui, T. Ema, *J. Am. Chem. Soc.* **2018**, *140*, 5334; c) D. Niu, L. Ji, G. Ouyang, M. Liu, *ACS Appl. Mater. Interfaces* **2020**, *12*, 18148; d) A. H. G. David, R. Casares, J. M. Cuerva, A. G. Campaña, V. Blanco, *J. Am. Chem. Soc.* **2019**, *141*, 18064.

[6] a) D. Niu, Y. Jiang, L. Ji, G. Ouyang, M. Liu, *Angew. Chem. Int. Ed.* **2019**, *58*, 5946; *Angew. Chem.* **2019**, *131*, 6007; b) H. Maeda, Y. Bando, K. Shimomura, I. Yamada, M. Naito, K. Nobusawa, H. Tsumatori, T. Kawai, *J. Am. Chem. Soc.* **2011**, *133*, 9266; c) H. Isla, M. Srebro-Hooper, M. Jean, N. Vanthuyne, T. Roisnel, J. L. Lunkley, G. Muller, J. A. G. Williams, J. Autschbach, J. Crassous, *Chem. Commun.* **2016**, *52*, 5932; d) A. Homberg, E. Brun, F. Zinna, S. Pascal, M. Górecki, L. Monnier, C. Besnard, G. Pescitelli, L. Di Bari, J. Lacour, *Chem. Sci.* **2018**, *9*, 7043; e) P. Reiné, A. M. Ortuño, S. Resa, L. Á. de Cienfuegos, V. Blanco, M. J. Ruedas-Rama, G. Mazzeo, S. Abbate, A. Lucotti, M. Tommasini, S. Guisán-Ceinos, M. Ribagorda, A. G. Campaña, A. Mota, G. Longhi, D. Miguel, J. M. Cuerva, *Chem. Commun.* **2018**, *54*, 13985; f) Y. Imaia, J. Yuasa, *Chem. Commun.* **2019**, *55*, 4095.

[7] a) J.-L. Ma, Q. Peng, C.-H. Zhao, *Chem. Eur. J.* **2019**, *25*, 15441; b) Y. Gao, C. Ren, X. Lin, T. He, *Front. Chem.* **2020**, *8*, 458; c) L. Zhang, H.-X. Wang, S. Li, M. Liu, *Chem. Soc. Rev.* **2020**, *49*, 9095; d) Y. Wu, L. H. You, Z.-Q. Yu, J.-H. Wang, Z. Meng, Y. Liu, X.-S. Li, K. Fu, X.-K. Ren, B. Z. Tang, *ACS Mater. Lett.* **2020**, *2*, 505; e) T. Zhao, J. Han, X. Jin, Y. Liu, M. Liu, P. Duan, *Angew. Chem. Int. Ed.* **2019**, *58*, 4978; *Angew. Chem.* **2019**, *131*, 5032; f) K. Takaishi, K. Iwachido, T. Ema, *J. Am. Chem. Soc.* **2020**, *142*, 1774; g) J. Han, P. Duan, X. Li, M. Liu, *J. Am. Chem. Soc.* **2017**, *139*, 9783; h) X. Yang, M. Zhou, Y. Wang, P. Duan, *Adv. Mater.* **2020**, *32*, 2000820.

[8] a) W. Wang, L.-J. Chen, X.-Q. Wang, B. Sun, X. Li, Y. Zhang, J. Shi, Y. Yu, L. Zhang, M. Liu, H.-B. Yang, *Proc. Natl. Acad. Sci. USA* **2015**, *112*, 5597; b) X.-Q. Wang, W.-J. Li, W. Wang, H.-B. Yang, *Chem. Commun.* **2018**, *54*, 13303; c) M. He, L. Chen, B. Jiang, H. Tan, C. Wang, H. Yang, *Chin. Chem. Lett.* **2019**, *30*, 131; d) W.-J. Li, Z. Hu, L. Xu, X.-Q. Wang, W. Wang, G.-Q. Yin, D.-Y. Zhang, Z. Sun, X. Li, H. Sun, H.-B. Yang, *J. Am. Chem. Soc.* **2020**, *142*, 16748.

[9] a) J. Liu, H. Su, L. Meng, Y. Zhao, C. Deng, J. C. Y. Ng, P. Lu, M. Faisal, J. W. Y. Lam, X. Huang, H. Wu, K. S. Wong, B. Z. Tang, *Chem. Sci.* **2012**, *3*, 2737; b) H.-T. Feng, C. Liu, Q. Li, H. Zhang, J. W. Y. Lam, B. Z. Tang, *ACS Mater. Lett.* **2019**, *1*, 192; c) F. Song, Z. Zhao, Z. Liu, J. W. Y. Lam, B. Z. Tang, *J. Mater. Chem. C* **2020**, *8*, 3284; d) M. Hu, H.-T. Feng, Y.-X. Yuan, Y.-S. Zheng, B. Z. Tang, *Coord. Chem. Rev.* **2020**, *416*, 213329; e) A. Nitti, D. Pasini, *Adv. Mater.* **2020**, *32*, 1908021; f) M.-M. Zhang, X.-Y. Dong, Z.-Y. Wang, H.-Y. Li, S.-J. Li, X. Zhao, S.-Q. Zang, *Angew. Chem. Int. Ed.* **2020**, *59*, 10052; *Angew. Chem.* **2020**, *132*, 10138; g) H. Wu, X. He, B. Yang, C.-C. Li, L. Zhao, *Angew. Chem. Int. Ed.* **2021**, *60*, 1535; *Angew. Chem.* **2021**, *133*, 1559.

[10] a) J. He, B. Xu, F. Chen, H. Xia, K. Li, L. Ye, W. Tian, *J. Phys. Chem. C* **2009**, *113*, 9892; b) B. Xu, W. Tian, *Aggregation-Induced Emission: Materials and Applications*, *Vol. 1*, American Chemical Society, Washington, **2016**, chap. 7, p. 113; c) X.-Q. Wang, W. Wang, W.-J. Li, Y. Qin, G.-Q. Yin, W.-L. Jiang, X. Li, S. Wu, H.-B. Yang, *Org. Chem. Front.* **2019**, *6*, 1686; d) Y. Dong, B. Xu, J. Zhang, X. Tan, L. Wang, J. Chen, H. Lv, S. Wen, B. Li, L. Ye, B. Zou, W. Tian, *Angew. Chem. Int. Ed.* **2012**, *51*, 10782; *Angew. Chem.* **2012**, *124*, 10940; e) Q. Qi, C. Li, X. Liu, S. Jiang, Z. Xu, R. Lee, M. Zhu, B. Xu, W. Tian, *J. Am. Chem. Soc.* **2017**, *139*, 16036.

[11] a) T. Ogoshi, S. Kanai, S. Fujinami, T. Yamagishi, Y. Nakamoto, *J. Am. Chem. Soc.* **2008**, *130*, 5022; b) T. Ogoshi, T. Akutsu, D. Yamafuji, T. Aoki, T.-a. Yamagishi, *Angew. Chem. Int. Ed.* **2013**, *52*, 8111; *Angew. Chem.* **2013**, *125*, 8269; c) T. Ogoshi, T.-a. Yamagishi, Y. Nakamoto, *Chem. Rev.* **2016**, *116*, 7937; d) T. Kakuta, T.-a. Yamagishi, T. Ogoshi, *Acc. Chem. Res.* **2018**, *51*, 1656; e) S. Fa, T. Kakuta, T.-a. Yamagishi, T. Ogoshi, *Chem. Lett.* **2019**, *48*, 1278; f) H. Zhu, Q. Li, B. Shi, H. Xing, Y. Sun, S. Lu, L. Shangguan, X. Li, F. Huang, P. J. Stang, *J. Am. Chem. Soc.* **2020**, *142*, 17340; g) J. Yao, W. Wu, W. Liang, Y. Feng, D. Zhou, J. J. Chruma, G. Fukuhara, T. Mori, Y. Inoue, C. Yang, *Angew. Chem. Int. Ed.* **2017**, *56*, 6869; *Angew. Chem.* **2017**, *129*, 6973; h) H. Zhu, Q. Li, Z. Gao, H. Wang, B. Shi, Y. Wu, L. Shangguan, X. Hong, F. Wang, F. Huang, *Angew. Chem. Int. Ed.* **2020**, *59*, 10868; *Angew. Chem.* **2020**, *132*, 10960.

[12] Selected reports on anion-induced wheel motions in (thio)urea-based rotaxanes: a) Y.-L. Huang, W.-C. Hung, C.-C. Lai, Y.-H. Liu, S.-M. Peng, S.-H. Chiu, *Angew. Chem. Int. Ed.* **2007**, *46*, 6629; *Angew. Chem.* **2007**, *119*, 6749; b) S.-Y. Hsueh, C.-T. Kuo, T.-W. Lu, C.-C. Lai, Y.-H. Liu, H.-F. Hsu, S.-M. Peng, C.-h. Chen, S.-H. Chiu, *Angew. Chem. Int. Ed.* **2010**, *49*, 9170; *Angew. Chem.*

2010, *122*, 9356; c) L. Liu, Y. Liu, P. Liu, J. Wu, Y. Guan, X. Hu, C. Lin, Y. Yang, X. Sun, J. Ma, L. Wang, *Chem. Sci.* **2013**, *4*, 1701; d) J. Berná, C. Franco-Pujantea, M. Alajarín, *Org. Biomol. Chem.* **2014**, *12*, 474; e) L. Liu, Q. Wang, M. Cheng, X.-Y. Hu, J. Jiang, L. Wang, *Asian J. Org. Chem.* **2015**, *4*, 221; f) T. A. Barendt, I. Rašović, M. A. Lebedeva, G. A. Farrow, A. Auty, D. Chekulaev, I. V. Sazanovich, J. A. Weinstein, K. Porfyrakis, P. D. Beer, *J. Am. Chem. Soc.* **2018**, *140*, 1924; g) X.-Q. Wang, W. Wang, W.-J. Li, L.-J. Chen, R. Yao, G.-Q. Yin, Y.-X. Wang, Y. Zhang, J. Huang, H. Tan, Y. Yu, X. Li, L. Xu, H.-B. Yang, *Nat. Commun.* **2018**, *9*, 3190; h) X.-Q. Wang, W.-J. Li, W. Wang, J. Wen, Y. Zhang, H. Tan, H.-B. Yang, *J. Am. Chem. Soc.* **2019**, *141*, 13923; i) W.-J. Li, W. Wang, X.-Q. Wang, M. Li, Y. Ke, R. Yao, J. Wen, G.-Q. Yin, B. Jiang, X. Li, P. Yin, H.-B. Yang, *J. Am. Chem. Soc.* **2020**, *142*, 8473; j) W.-J. Li, X.-Q. Wang, W. Wang, Z. Hu, Y. Ke, H. Jiang, C. He, X. Wang, Y.-X. Hu, P.-P. Jia, P. Yin, J. Chen, H. Sun, Z. Sun, L. Xu, H.-B. Yang, *Giant* **2020**, *2*, 100020.

[13] Selected reports on switchable chiral information transfer in rotaxanes: a) M. Asakawa, G. Brancato, M. Fanti, D. A. Leigh, T. Shimizu, A. M. Z. Slawin, J. K. Y. Wong, F. Zerbetto, S. Zhang, *J. Am. Chem. Soc.* **2002**, *124*, 2939; b) G. Bottari, D. A. Leigh, E. M. Pérez, *J. Am. Chem. Soc.* **2003**, *125*, 13360; c) F. Ishiwari, K. Nakazono, Y. Koyama, T. Takata, *Angew. Chem. Int. Ed.* **2017**, *56*, 14858; *Angew. Chem.* **2017**, *129*, 15054; d) M. Gaedke, F. Witte, J. Anhäuser, H. Hupatz, H. V. Schröder, A. Valkonen, K. Rissanen, A. Lützen, B. Paulus, C. A. Schalley, *Chem. Sci.* **2019**, *10*, 10003.

[14] Selected reports on pillar[5]arene-based (*pseudo*)[3]rotaxanes: a) H. Chong, C. Nie, L. Wang, S. Wang, Y. Han, Y. Wang, C. Wang, C. Yan, *Chin. Chem. Lett.* **2021**, *32*, 57; b) J. Ye, R. Zhang, W. Yang, Y. Han, H. Guo, J. Xie, C. Yan, Y. Yao, *Chin. Chem. Lett.* **2020**, *31*, 1550; c) J.-D. Ding, J.-F. Chen, Q. Lin, H. Yao, Y.-M. Zhang, T.-B. Wei, *Polym. Chem.* **2018**, *9*, 5370; d) L. Ma, S. Wang, C. Li, D. Cao, T. Li, X. Ma, *Chem. Commun.* **2018**, *54*, 2405; e) T. Ogoshi, D. Yamafuji, T. Aoki, K. Kitajima, T.-a. Yamagishi, Y. Hayashi, S. Kawauchi, *Chem. Eur. J.* **2012**, *18*, 7493.

[15] Deposition Number 2048250 (for [3]rotaxane **1**) contains the supplementary crystallographic data for this paper. These data are provided free of charge by the joint Cambridge Crystallographic Data Centre and Fachinformationszentrum Karlsruhe Access Structures service www.ccdc.cam.ac.uk/structures.

[16] a) A. J. Lowe, G. A. Dyson, F. M. Pfeffer, *Org. Biomol. Chem.* **2007**, *5*, 1343; b) A. J. Lowe, G. A. Dyson, F. M. Pfeffer, *Eur. J. Org. Chem.* **2008**, 1559.

[17] a) V. Bernard, *Molecular Fluorescence Principles and Applications*, Wiley-VCH, Weinheim, **2002**; b) J. Zhang, B. Xu, J. Chen, S. Ma, Y. Dong, L. Wang, B. Li, L. Ye, W. Tian, *Adv. Mater.* **2014**, *26*, 739.

[18] a) P. J. Stephens, F. J. Devlin, C. F. Chabalowski, M. J. Frisch, *J. Phys. Chem.* **1994**, *98*, 11623; b) T. Yanai, D. P. Tew, N. C. Handy, *Chem. Phys. Lett.* **2004**, *393*, 51; c) W. Zhang, J. Liu, X. Jin, X. Gu, X. C. Zeng, X. He, H. Li, *Angew. Chem. Int. Ed.* **2020**, *59*, 11550; *Angew. Chem.* **2020**, *132*, 11647; d) L. W. Chung, W. M. C. Sameera, R. Ramozzi, A. J. Page, M. Hatanaka, G. P. Petrova, T. V. Harris, X. Li, Z. Ke, F. Liu, H. B. Li, L. Ding, K. Morokuma, *Chem. Rev.* **2015**, *115*, 5678; e) A. K. Rappé, C. J. Casewit, K. S. Colwell, W. A. Goddard, W. M. Skiff, *J. Am. Chem. Soc.* **1992**, *114*, 10024.

[19] J. P. Riehl, F. S. Richardson, *Chem. Rev.* **1986**, *86*, 1.

[20] a) E. M. G. Jamieson, F. Modicom, S. M. Goldup, *Chem. Soc. Rev.* **2018**, *47*, 5266; b) N. Pairault, J. Niemeyer, *Synlett* **2018**, *29*, 689; c) N. H. Evans, *Chem. Eur. J.* **2018**, *24*, 3101; d) K. Nakazono, T. Takata, *Symmetry* **2020**, *12*, 144; e) C. Tian, S. D. P. Fielden, B. Pérez-Saavedra, I. J. Vitorica-Yrezabal, D. A. Leigh, *J. Am. Chem. Soc.* **2020**, *142*, 9803.

Manuscript received: January 20, 2021
Revised manuscript received: February 7, 2021
Accepted manuscript online: February 9, 2021
Version of record online: March 11, 2021